Comments on methods of analyses of nucleon-nucleus scattering data

K. Amos[1*]

School of Physics, University of Melbourne, Victoria 3010, Australia

S. Karataglidis[2†]

Department of Physics, University of Johannesburg, P.O. Box 524, Auckland Park, 2006, South Africa

(Dated: July 5, 2010)

Abstract

Methods of analysis of nucleon-nucleus scattering data have progressed markedly over the past 50 years, yet many analyses of scattering data still use prescriptions specified at various stages of that progress. But the assumptions made or inherent in those analyses are poorly justified and most are no longer necessary to facilitate evaluations. We investigate some of those assumptions and highlight deficiencies and the uncertainties they may make in data analyses.

PACS numbers:

*Electronic address: amos@physics.unimelb.edu.au

†Electronic address: stevenka@ac.uj.za

I. INTRODUCTION

An ultimate aim of a nuclear reaction theory is to probe details of the structure of the nuclei involved. There are many and diverse reactions and observables one might use in that quest but herein we consider just cases of nucleon scattering (elastic and inelastic), focussing upon questions that need be raised regarding methods of analyses used. The questions raised apply to various extent to theories for the scattering and reactions involving other nuclear projectiles.

First we deal with the problem of elastic scattering of nucleons. It is of great regret that many assume that elastic scattering data are not of interest experimentally or theoretically. But almost all theories of nucleon-nucleus reactions presume a knowledge of the elastic scattering data for the system. It is commonly thought that such can be approximated by using some global, phenomenological, local optical model potential. But in doing so, there are uncertainties that may vitiate using a reaction theory for data analysis to achieve the prime purpose of assessing the structure of the target.

For many years analyses of experimental data from reactions initiated by nucleons, by protons mostly, have been of interest, in part as the incident proton most strongly interacts with neutrons in the target. Analyses of proton scattering data then complement those of electron scattering form factors which are more sensitive to the proton distributions in nuclei. If, as well, static moments and electromagnetic transition rates are known, the body of data could well assess putative details of low energy structures of nuclei. However, the methods of data analysis used need be of comparable surety for any conclusions drawn to have sufficient credibility. But one must bear in mind that electromagnetic transition rates, electron scattering form factors, and nucleon scattering data can be sensitive to disparate aspects of the nuclear wave functions so that a model of structure may be adequate for some data analyses and not others. Now while the theories used to analyze electromagnetic data are well established, with the size, if not specific influence, of corrections to results found known, that is not the case with most theories used to analyze nucleon-induced reactions.

To date analyses of data from nucleon induced reactions can only be made using significant approximations to a basic theory of such scattering. In doing so, guidance from some physical properties and physics principles are needed to justify whatever model theory of the reaction is used. It is an evolutionary process and one can only assess approximations used in the past against results from another developed theory in which such approximations have not been made or are of lesser influence. To date, of course, all applicable theories of nuclear scattering involve approximations. Still, by treating the system more assiduously, it is possible to understand why conclusions drawn from past analyses need be treated cautiously and not taken as definitively as authors may have indicated.

For analyses of nucleon-nucleus elastic scattering data, the first theoretical approach was phenomenological, dating back to Bethe [1]. The form chosen for the associated optical model potentials was taken to reflect the expected density distribution of nucleons in each target nucleus. Subsequently, optical potential was sought microscopically, folding a free nucleon-nucleon interaction with a density profile for the target. The most well known of those approaches was that of Kerman, McManus, and Thaler (KMT) [2]. Later formulations took into account medium corrections to the interaction between the incident nucleon with those bound in the target as well as specifically including the nonlocality arising from exchange amplitudes associated with treatment of the Pauli principle. Those g-folding models are discussed in detail in a review [3].

All of the models identified in the above, and various sets with intermediate steps (such as the JLM approach [4]) have been, and continue to be, used to analyse scattering data. What we present is not intended as a justification of the most recent applications. Rather we seek to point out the inadequacies of the models formed in distinct stages of development, why some should no longer be used, and why the conclusions drawn from the use of many be treated with more caution.

II. THE OPTICAL MODEL POTENTIALS

Most optical potentials used are of local type, whether they be defined phenomenologically (usually with Woods-Saxon form) or by folding schemes. Typical of the latter is the JLM method as recently used [5], in which the direct (local) term is found by folding an NN interaction with the nucleon density profile of the target. The imaginary term is specified phenomenologically. Some also account approximately for the exchange process arising from the indistinguishability of the projectile with the nucleons bound in the target by using an additional local term. But there are problems with all of these approaches, and especially in using the relative motion wave functions generated from local optical potentials.

A. On fitting elastic scattering data

A primary problem, and a rather insidious one, is that justification of an optical potential is founded upon finding a fit to elastic scattering data: cross sections and spin observables. Of course, a viable optical potential in a single channel theory of elastic scattering should indeed provide such fits. But does a fit to such data imply a proper (the "correct") optical potential? Many assume that the answer to the question is yes. Few, it seems, fully appreciate the limited validity of such a justification.

A fit to elastic scattering data only requires that the scattering theory produce a set of phase shifts that, when used in the standard sums of Legendre polynomials, give a good fit to data. In no way is that a proof of the uniqueness of the phase shifts, and even less of the interactions used in the Schrödinger equations producing them. Of course, a "proper" optical potential must lead to a good set of phase shifts, and as well a fit to measured elastic scattering data, but in specifying the interaction, one must use as many principles of physics as possible to have maximal credibility. Basically, all the usual phenomenological and part phenomenological models that end with purely local forms for a nucleon-nucleus optical potential fail in that respect to some extent. To get elastic scattering phase shifts only requires knowledge of the relative motion wave functions and their derivatives at extreme separation of the nucleon and nucleus. How those wave functions attained the required asymptotic properties from solutions of Schrödinger equations is not defined by those numbers alone.

Given a set of phase shifts that typically are necessary to have an excellent fit to data, such as with the elastic scattering of 200 MeV protons from ^{12}C, phenomenological potentials, potentials from inverse scattering theories, and those microscopically formed (g-folding) all exist from which quality fits to the same data have been found. Some of those fits are associated with a chi-squared per degree of freedom (χ^2/F) values ~ 1.

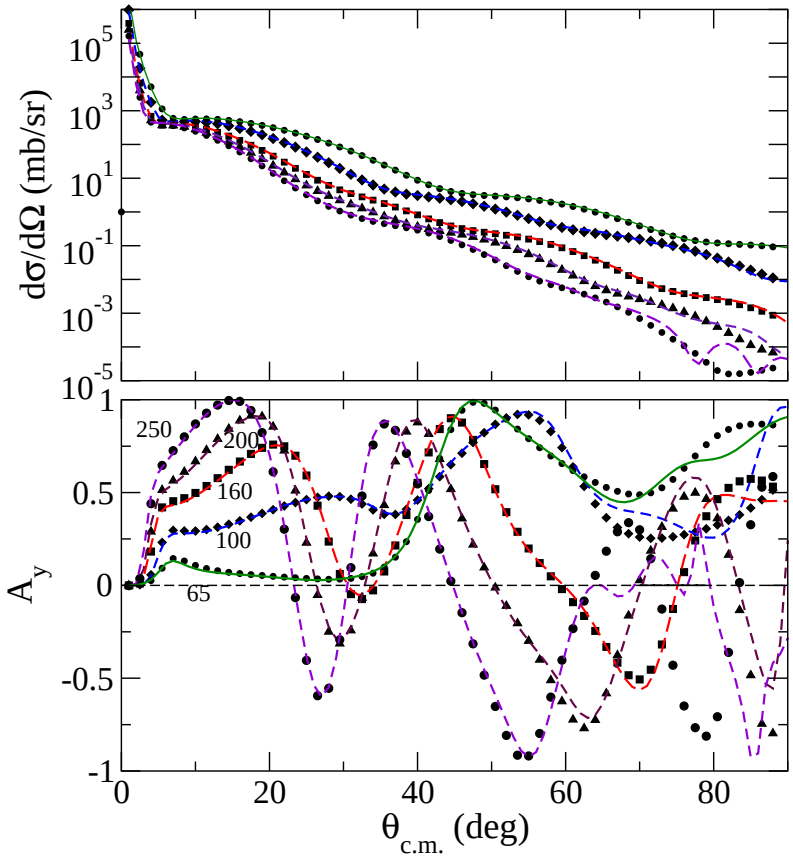

FIG. 1: (Color online) Comparisons of the differential cross sections (top) and analyzing powers (bottom) from defined sets of phase shifts with those deduced by using their inversion potentials.

1. *An example of equivalent optical potentials*

The conventional approach, the phenomenological optical model potential approach, to analyses of elastic scattering data is an example of inverse scattering. Specifically it is an example of numerical inverse scattering: the fit to data determines values of the parameters deemed best. More generally, the inverse scattering problem for fixed energy scattering resolves to the following: *Given an S-function (phase shifts) at a particular energy, find local central and spin-orbit potentials that reproduce that S-function when used in Schrödinger equations.* One fully quantal method to do that is the modified Newton-Sabatier scheme [6] which finds potentials of the Bargmann class. That approach has been used with sets of phase shifts (the "data") obtained from a microscopic (g-folding) model of the elastic scattering of protons at energies of 65, 100, 160, 200 and 250 MeV from ^{12}C. The cross sections and spin measurables found therefrom [3] are in very good agreement with actual measured data. For comparison, those phase shifts have been used as input to the inversion scheme [6] to find a set of local (Schrödinger) potentials [7]. The (complex, central and spin-orbit) potentials were then used in Schrödinger equations to find if the same set of phase shifts would be regenerated. The cross sections and analyzing powers from the g-folding model are shown by the symbols in Fig. 1 while those resulting from use of the determined (local) inversion potentials are shown by the various dashed lines. Clearly the reproductions are very good

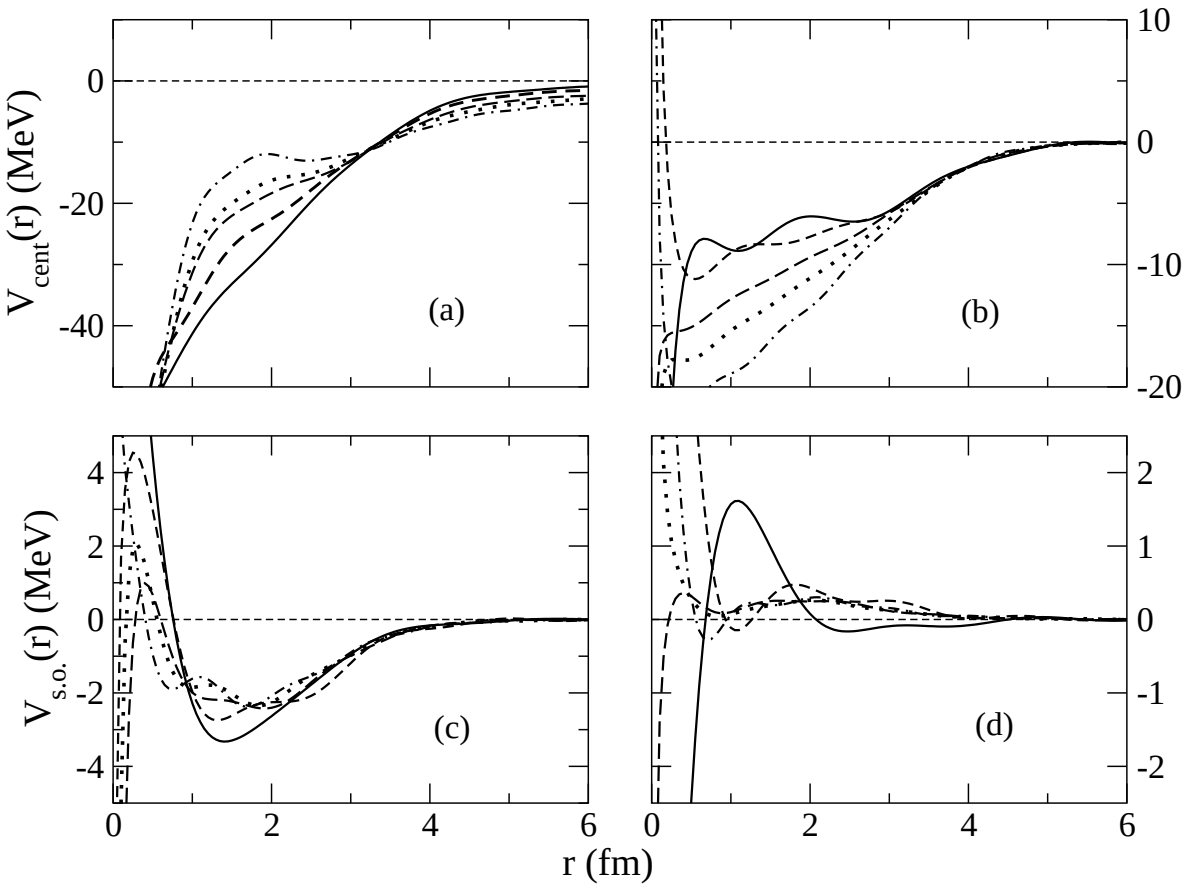

FIG. 2: The potentials defined by using a modified Newton-Sabatier inversion scheme with the set of phase shifts for 65 to 250 MeV protons on ^{12}C.

with but a minor mismatch for 250 MeV at large ($\theta \geq 70°$) scattering angles.

The potentials obtained from modified Newton-Sabatier inversion calculations are displayed in Fig. 2. Therein the central real, central imaginary, spin-orbit real, and spin-orbit imaginary terms are displayed in panels labelled (a), (b), (c), and (d) respectively. The potentials for energies 65, 100, 160, 200, and 250 MeV are portrayed by the solid, dashed, long-dashed, dotted, and dot-dashed curves respectively. The energy dependence resulting with these interactions clearly is severe. The central potentials become less refractive and more absorptive with increase in energy. The spin-orbit interactions vary even more markedly. These local potential forms determined by quantal inverse scattering theory are distinctly different from the Woods-Saxon interactions usually taken with the phenomenological optical. But they fit the "data" (and from the origins, the actual measured data) very well. Indeed, a criterion was that the inversion process must give "data" fits with measure χ^2/degree of freedom of $\mathcal{O}(1)$.

The actual cross section data [8] for the elastic scattering of 200 MeV protons on ^{12}C are numerous and of high quality. The basic Newton-Sabatier method has been used [9] to ascertain local complex potentials from them. Two distinct inversion potentials have been found. They are shown in the right panel of Fig. 3; the real parts in the top and the imaginary ones in the bottom segments. The loop was completed by using both potentials in Schrödinger equations whose solutions gave phase shifts, and then the scattering cross

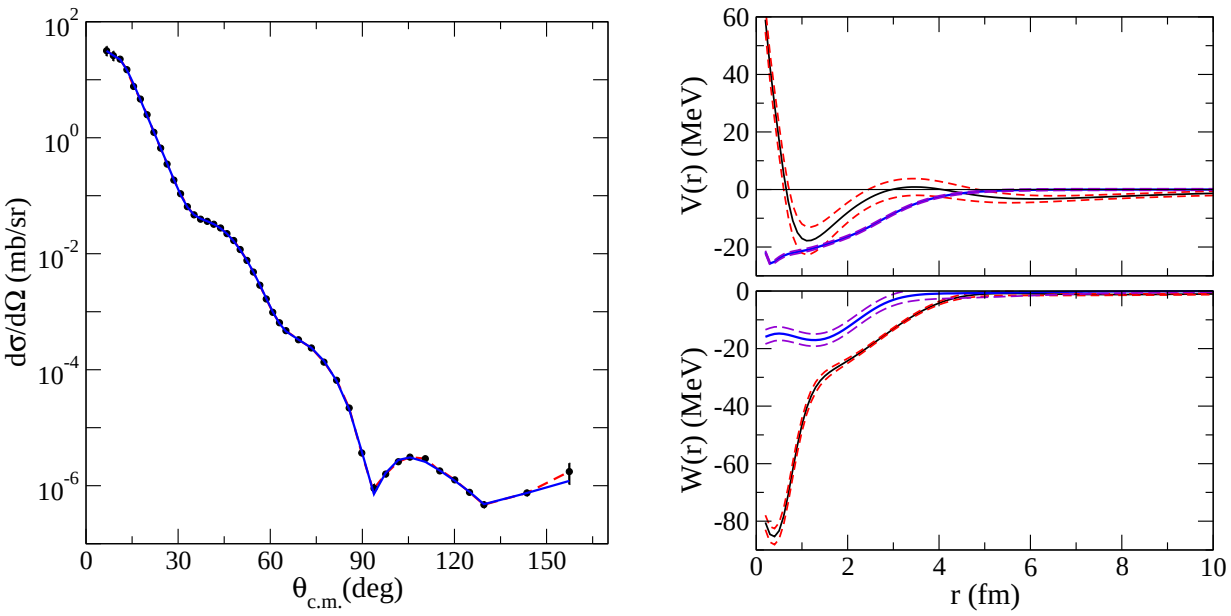

FIG. 3: (Color online) The data from the elastic scattering of 200 MeV protons on ^{12}C compared with cross sections determined from two inversion potentials (left panel). The two potentials are depicted, as functions of radius in the right panel. The real and imaginary parts are shown in the top and bottom segments respectively with their bands of confidence indicated. Details are given in the text.

sections that are compared with the actual data in the left panel of Fig. 3. The evaluated cross sections are practically indistinguishable from the data reflecting that the two results fit the data with values of χ^2/degree of freedom 1.006 and 1.018. The two calculated cross sections differ only in the region of the largest scattering angle, and then but slightly.

The two distinctive potentials were found from two sets of pole-zero pairs that represent the S-function that one needs first for the chosen inverse scattering theory. Details are given in Ref. [9]. The approach allows specification of bands of confidence on those potentials. They are shown in Fig. 3 by the dashed curves surrounding the potentials. Those bands, determined from an error analysis [9], are to be interpreted as follows: should another potential exist associated with a fit to the data with the same χ^2/F, then there is a 60% chance that it would lie within that band. Clearly then, as the two cases shown are so different, even such good data are insufficient to delineate a potential uniquely. To these one might add any finely tuned phenomenological model form. Thus a claim that a nucleon-nucleus interaction is the correct one, based solely upon its fit to elastic scattering data, is not valid. A "correct" potential must be based upon more physical information. Simply linking its form to expected matter and charge distributions of the nucleus is not sufficient in this regard, however.

B. The effect of the Pauli principle

A problem with most single channel (optical model) potentials is that they are local in form. Those defined fully, or in part, phenomenologically usually take parametric forms and values in accord with some notions regarding the matter and/or charge distributions of

nucleons in the targets. The charge distribution of the targets may be well reflected by the form factor from the elastic scattering of electrons but one cannot assume that the matter distribution is then necessarily as well-described. This is most evident when describing scattering from or by neutron halo nuclei [10]. Certainly the elastic scattering of nucleons does not directly justify parameter forms for the reasons discussed above.

One may hold faith in the neutron distributions given by large basis models of the ground state structure of any nucleus at least inside and near to the nuclear surface. Indeed, their use in folding NN-interactions to form an NA optical potential lead to results in good agreement with elastic scattering observables. But, in so doing, unlike the case of electron scattering, one must also take into account effects of the Pauli Principle. The prime effect of that principle in defining NA optical potentials in the microscopic approach built essentially on KMT theory [2], is to make the interaction highly nonlocal. That nonlocality is associated with the exchange amplitudes arising from the indistinguishability of the projectile with nucleons in the target. The contributions from scattering in which the detected (emergent) nucleon originally was bound within the target are extremely important. They must be treated carefully, since the associated (exchange) amplitudes have a different momentum transfer profile to the direct scattering ones. Even more critical is that, often, these exchange amplitudes destructively interfere with the direct ones. This has been demonstrated for a range of energies [11] so only an illustrative example is included herein. Cross sections from the elastic scattering of protons from ^{12}C at energies of 185 and 200 MeV are shown in Fig. 4. Masking of such effects in the fitting procedures of local phenomenological forms is insufficient. As discussed previously, such potentials are necessarily not unique.

The considerable effects of the exchange amplitudes indicate also that theories predicated upon just the charge and/or matter densities have a problem. The exchange amplitudes require input of the one-body density matrices which include, but contain more information than, the simple density. One needs explicit single nucleon wave functions in fact. The severe destructive interference noted also means that seeking equivalent local potentials to approximate such may be quite problematic.

C. Medium effects with the basic NN interaction

In the 1980's there was a watershed in the studies of NN and NA scattering. First, reliable NN scattering amplitudes were defined and detailed phase shift analyses [12] made, at least for energies up to the pion threshold. Second the Nijmegen [13], Paris [14], and Bonn [15] NN potentials were developed to fit those NN amplitudes and phase shifts. Also the status of microscopic NA optical potential theories was reviewed at a seminal topical workshop in Hamburg [16]. Finally, experimental studies in those years produced many and varied high quality NN data sets for energies to 1 GeV [17], adding impetus to implementations of the theories. Since that time reviews [3, 18] of the optical model for scattering have been made given the central role it plays in studies of nucleon-induced reactions [19–21].

Standard now is the optical potential built upon non-relativistic multiple scattering theory with the NN scattering amplitudes modified from the free NN values. The result is an *effective NN interaction*. Those modifications are caused by the two nucleons interacting within the nuclear medium and are due to *Pauli blocking* and *mean field* effects for both projectile and bound state nucleons. In addition, there are other effects due to the convolution of the NN scattering amplitudes with target structure that require off-the-energy-shell

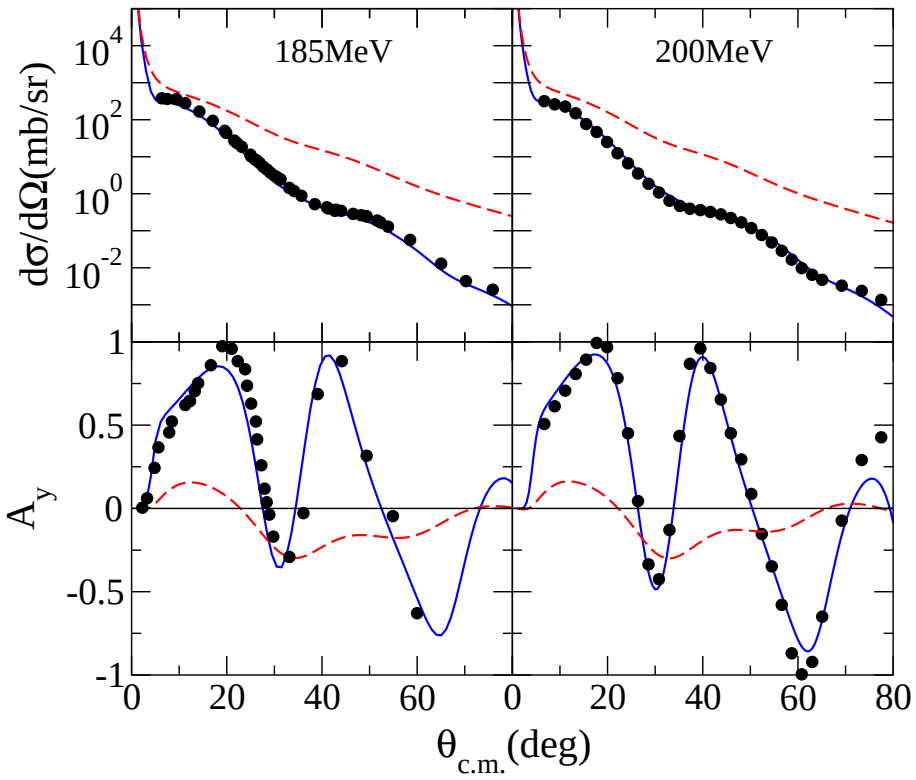

FIG. 4: (Color online) Differential cross sections (top) and analyzing powers (bottom) from the elastic scattering of 185 (left) and 200 MeV (right) protons with ^{12}C. The solid curves are the results found using a complete g-folding model optical potential while the dashed curves are the results obtained by omitting the nonlocal exchange parts of those interactions.

scattering amplitudes. Also of importance is the complete antisymmetrization (at least at the two nucleon level) of the $A+1$ nucleon scattering system which leads to direct and knock-out (exchange) amplitudes for NA scattering. As illustrated before, the effect of such NA exchange amplitudes is not small at any energy and those amplitudes are a major source of nonlocality. Other medium effects [22] also can have some significance. Details of the forming the effective interactions from a chosen free NN interaction are given in the review [3]. We have used both the Paris and the BonnB interactions in our evaluations of NN t-matrices and NN g-matrices; the choice gives only small differences in results.

In Fig. 5 the effects that medium dependence of the NN effective interaction have in the cross sections and analyzing powers are shown. Results for the elastic scattering of 65 MeV protons from ^{40}C are shown in the left panel while those from ^{208}Pb are given in the right panel. The data [23] are shown by the filled circles while the calculated results found using g-folding potentials are depicted by the solid curves. The results shown by the dashed curves are from optical potentials having no density dependence in the effective interaction, i.e. formed by folding the free NN t-matrices. The density matrices for ^{40}Ca used in forming the folding potentials were taken from SHF (Skyrme-Hartree-Fock) calculations [24] while those for ^{208}Pb were from a simple packed shell model with oscillator wave functions ($\hbar\omega = 6.7$ MeV).

The role of density dependence in the NN effective interactions is very evident, most notably in the analyzing power results. Density dependence clearly improves agreement

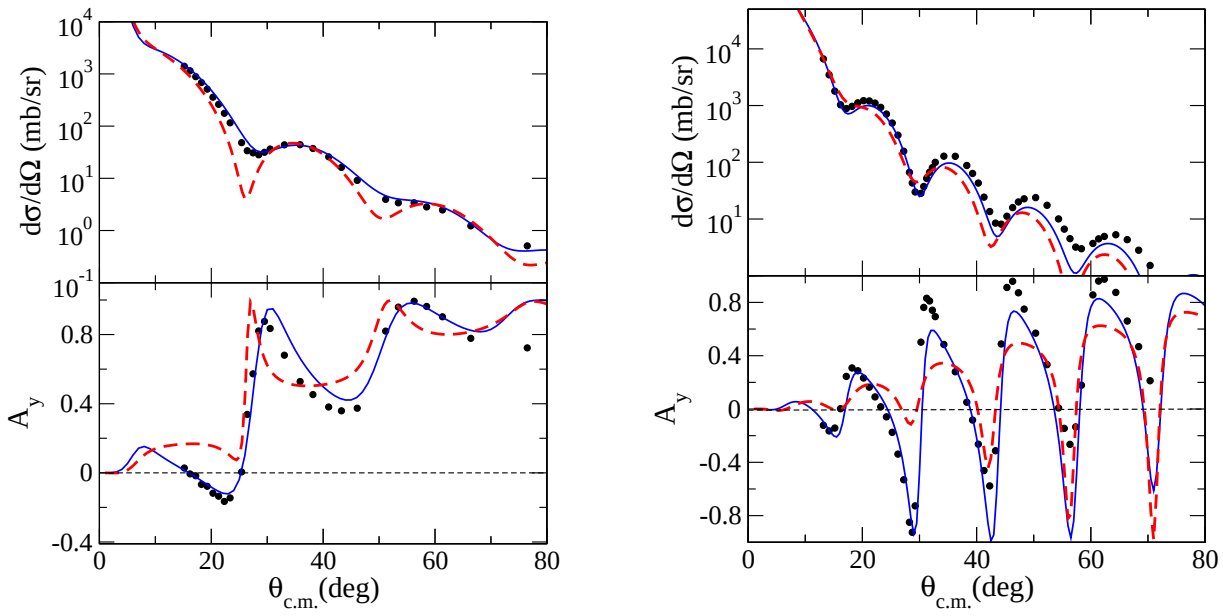

FIG. 5: (Color online) Elastic scattering cross sections and analyzing powers for 65 MeV protons scattering from ^{40}Ca (left) and from ^{208}Pb (right). The solid curves are the results of using the density dependent, NN g-matrices in forming the optical potentials, while the dashed curves are the results found using the free NN t-matrices in the folding process.

with the data in both cases. However, it is apparent that the ^{208}Pb results are not in as good agreement with the data as are the ^{40}Ca ones. The issue is one of structure as is shown next in Fig. 6. In this figure, cross sections from the elastic scattering of 65 MeV nucleons from ^{208}Pb are shown. The data from proton scattering [23] and from neutron scattering [25] are compared with results from g-folding potentials found using two different models of the nuclear wave functions. The dashed curves are results given by a packed shell model with proton oscillators of $\hbar\omega = 6.7$ MeV as before, but $\hbar\omega = 7.25$ MeV was used for the neutrons. This gave a neutron skin thickness ($S = 0.16$ fm), comparable to that of an SHF calculation [24]. The solid curves in the figure result when SHF model wave functions are used to specify the g-folding potentials. The neutron scattering cross sections are quite well reproduced by both calculated results but the proton scattering results indicate a preference for the SHF model input. This reflects primarily the difference in the neutron distributions given by the two models of structure.

Of course, by judicious adjustment of parameter values in a purely phenomenological approach, even better fits to this data can be achieved. Such is shown in Fig. 7. The parameter values used were those defined by van Oers *et al.* [26] for 40 MeV protons incident on ^{208}Pb, and by Finlay *et al.* [27] for 40 MeV neutron scattering. Results found using the van Oers *et al.* potential for both scatterings are depicted by the solid curves while those found using the Finlay *et al.* potential are displayed by the dashed curves. The parameter values differ significantly as one may expect for nucleon scattering from $N \neq Z$ systems. For completeness those parameter values are given in Table I.

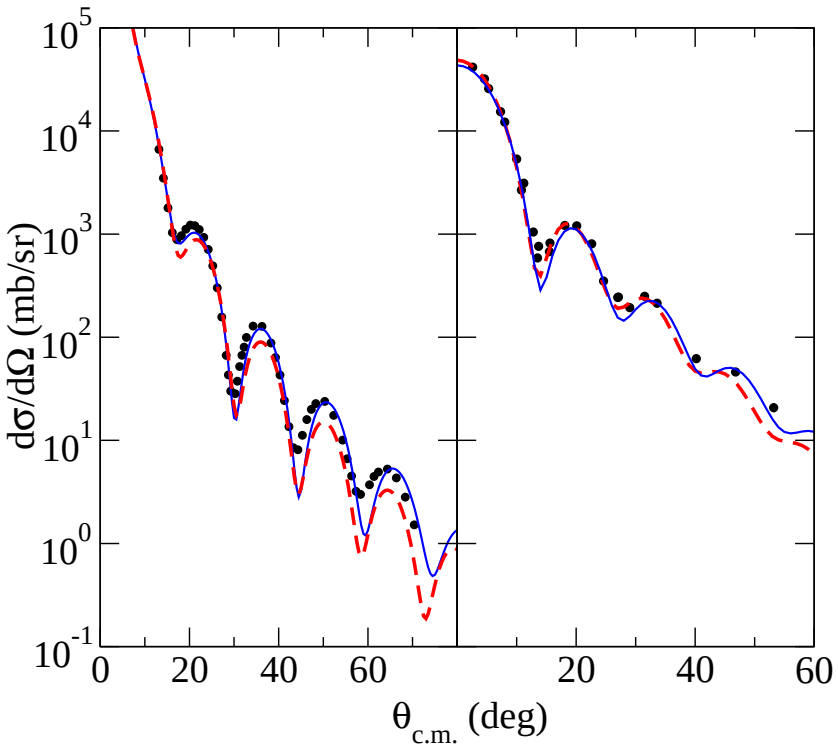

FIG. 6: (Color online) Cross sections for the elastic scattering of protons (left) and of neutrons (right) from ^{208}Pb.

TABLE I: The parameter values for the optical model potentials that lead to the fits to cross-section data shown in Fig. 7. Other specifics are given in Refs. [26] and [27]

term	40 MeV protons	40 MeV neutrons
V_0 (MeV)	51.8	36.73
r_0 (fm)	1.159	1.205
a_0 (fm)	0.784	0.685
W_0 (MeV)	3.98	5.2
W_D (MeV)	5.75	2.55
r_D (fm)	1.321	1.283
a_D (fm)	0.727	0.569
$V_{s.o.}$ (MeV)	6.66	5.75
$r_{s.o.}$ (fm)	1.044	1.105
$a_{s.o.}$ (fm)	0.905	0.499
r_c (fm)	1.05	

D. Energy dependence problems

The projectile energy dictates what approximations may be made to a 'full' scattering theory. At low values of incident energies, discrete state effects are known to influence scattering [28]. In those cases, a coupled-channel model of scattering is essential. An appro-

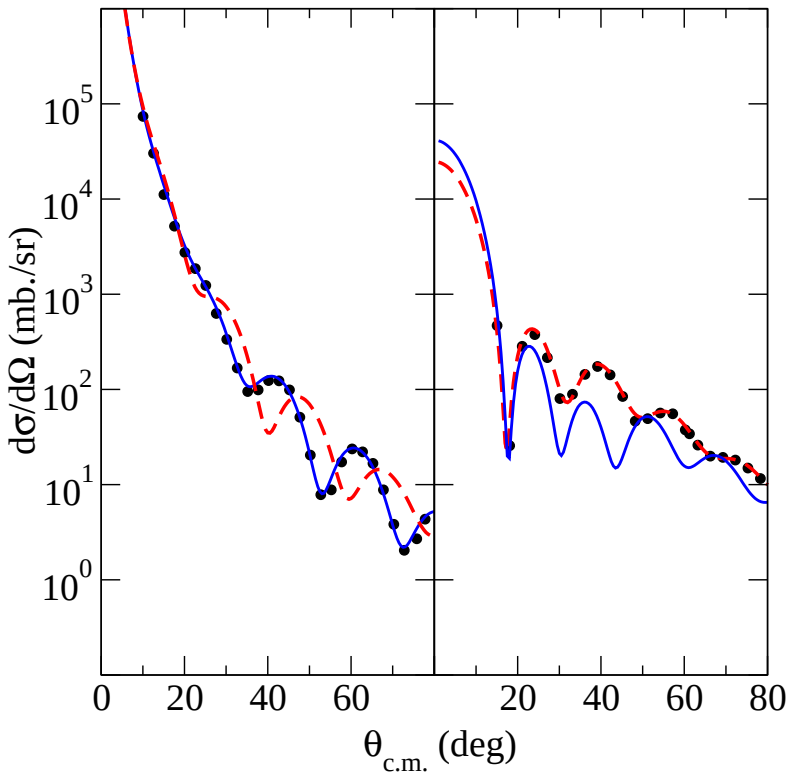

FIG. 7: (Color online) Cross sections for the elastic scattering of 40 MeV protons (left) and of 40 MeV neutrons (right) from ^{208}Pb, compared to results from using phenomenological optical model potentials.

priate one, which ensures that the Pauli principle is not violated even with a collective model prescription for the coupling, now exists and has been used to explain compound nucleus structure even in exotic, radioactive light mass systems [29]. Treating the Pauli principle adequately in coupled-channel calculations was crucial as shown in a comparative study of two coupled-channel evaluations [30].

Consider now, incident energies above any excitation energy value of giant resonances (if such exist in the target). Some time ago, it was shown that specific properties (the giant resonances) could dynamically influence proton scattering for energies of protons that coincide with their virtual excitation in the target [31]. For such incident energies there has been another coupled-channels method proposed [32]. That method, the continuum discretised coupled channel (CDCC) method, has been used with some success in analyses of break-up reactions for projectile energies similar to those we have used. Those successes might be considered indicative of a problem with the g-folding approach for nucleon elastic scattering. However, the discretization of the continuum is only a statistical one and is not based upon any attributes of the target continuum. Also the effects of the Pauli principle (projectile-bound nucleons) are not taken into account with the phenomenological optical potentials used. But there are other concerns with the CDCC method. As Deltuva *et al.* [33] noted: *"CDCC results obtained with two different basis sets, namely the basis set using the continuum of the projectile in the entrance channel, and the one using the continuum of the composite system in the final transfer channel, led to substantially different breakup cross sections for* $p(^{11}Be,^{10}Be)pn$. *These findings raise concern about the accuracy of the CDCC*

method, not only as a means to describe reaction dynamics, but also as an accurate tool to extract structure information on halo nuclei."

For medium energies, such as we consider herein, then such continuum coupling as well as coupling between the low excitation energies in the target are not expected to be important. Certainly there has been no need for such when a good model of structure and a reasonable NN force were used in evaluations. That is so at least for elastic scattering cross sections usually greater than about 0.1 mb/sr. We do not dispute a role of coupled channels in a scattering process, but we are convinced that such are a requirement in analyses of nucleon elastic scattering data only when there are specific (collective and not too spread) states in the target nucleus at excitation in the vicinity of the incident energy value. Likewise there can be other reaction processes contributing to a given transition, such as the formation of a virtual deuteron via a *p*-*d*-*p* chain as considered by some [34, 35]. But such second order terms, even if it is possible to effect a virtual deuteron and given the multiple final, possibly unbound, states to which the break-up could lead, should give small contribution in comparison to the direct ones in forming elastic scattering cross sections. Further the other problems as detailed before with either the modified JLM model or the CDCC coupling scheme that has been used [34, 36] make the estimates given for the virtual formation process unreliable. These problems detract from conclusions made in those papers on the structures of the nuclei involved.

Finally, as the incident nucleon energy increases to near and above the Delta resonance threshold in the NN frame, both that and other resonances need be taken into account in defining an effective NN interaction. Relativity also becomes an increasing issue, and one of more than a kinematic factor. However, below about 300 MeV, the non-relativistic g-folding results compare well with data and more than favorably with global Dirac potential model results [37].

III. INELASTIC SCATTERING OF NUCLEONS

Inelastic nucleon scattering data from excitation of discrete states in nuclei usually has been analysed using a DWA (distorted wave approximation). Coupled channels analyses also have been made, but they still are made using collective models of structure, usually with local coupled channel potentials. That localisation suffers from the same problems as does the local phenomenological or semi-phenomenological optical model potentials described previously.

For elastic scattering one only requires appropriate relative motion wave functions at large distances; appropriate meaning that they yield a set of suitable phase shifts. For non-elastic reaction evaluations, with the DWA, the relative motion wave functions need be specified through the nuclear volume. The choice of optical model form then is of serious concern.

A. Relative motion wave functions

The problem of not considering the effects outlined in the previous sections (Pauli blocking, mean-field effects, and nonlocality) extends to descriptions of nucleon-induced reactions for which the optical potential serves to define the effective interaction mediating the reaction. In that respect, an appropriate (physically justified) determination of the relative motion wave function (nucleon incident on the nucleus) is required in order to have confi-

dence in the description of the related reaction. In this subsection, we consider the relative motion wave functions associated with two optical model potentials. Specifically we compare the partial wave functions generated from a g-folding model [28] and those from a phenomenological potential whose parameters have been set to 'best fit' the same cross section data. As shown above in Fig. 6, g-folding model evaluations gave quite good fits to both the proton and neutron scattering cross sections. Even better fits to the data were obtained using phenomenological optical model potentials (see Fig 7). Essentially then both the microscopic and phenomenological potentials yield relative motion wave functions that are the same asymptotically. However, their relative motion wave functions differ through the volume of the nucleus.

Whatever be the (non-relativistic, spherical) nucleon-nucleus optical model potential, with the beam direction as the z axis, relative motion wave functions for neutrons are written in partial wave form

$$\Psi_\nu(\mathbf{k},\mathbf{r}) = \frac{1}{k}\sum_{l,j}\sqrt{4\pi(2l+1)}\, i^l f_{l,j}(kr)\left\langle l\ \frac{1}{2}\ 0\ \nu \mid j\ \nu\right\rangle \mathcal{Y}^\nu_{l\frac{1}{2}j}(\Omega_r), \tag{1}$$

where $\mathcal{Y}$ is the standard tensor spherical harmonic for a spin-$\frac{1}{2}$ function.

Consider the case of 40 MeV neutrons elastically scattered from ^{208}Pb. The relative motion wave functions for the s–, p–, and d– partial waves are displayed in Figs. 8, 9, and 10 respectively. The real and imaginary parts of those wave functions are shown on the left and right hand sides of the figures. The solid curves portray the wave functions generated by the nonlocal, microscopic g-folding optical potential while those found using the phenomenological potential [27] are shown by the dashed curves. All wave functions were obtained from specific runs of Raynal's updated version, DWBA98, of his code DWBA91 [38].

The effect of nonlocality upon s-wave relative motion wave functions through the nuclear volume, shown in Fig. 8, is to markedly decrease the real part while having a smaller decrease on the imaginary part of the wave function compared to that found using the (essentially phase equivalent) local potential model. The scaling is not the overall 10-15% that has often been assumed (the Perey effect [39, 40]).

The p- and d- wave functions are similarly effected, though in the case of the p-waves, it is with the imaginary part as given by the code, that the large size reduction due to nonlocality occurs.

To emphasise the difference between the wave functions associated with the two 'phase equivalent' interactions for 40 MeV neutrons on ^{208}Pb, the partial wave sum completed along the beam line (for which $\Omega_r = \pi$ for $z < 0$ and 0 thereafter, gave the magnitude of the spin up ($\nu = \frac{1}{2}$) scattering waves as displayed in Fig. 11.

As nuclear structure models, by virtue of the fact that they are models, do not precisely describe nuclei, there are mismatches between observed quantities and the values predicted. Whether that be γ-decay rates or inelastic scattering cross sections, a match is sought by using effective transition operators with the ensuing scaling of calculated results defined as 'core polarisation', which are considered in the next section. Nevertheless, the differences obtained in the relative motion wave functions when one considers the effects in scattering (Pauli blocking, nonlocality, etc.) illustrate the problem in describing nucleon-induced reactions and the correction factors that may be necessary *a posteriori*. Such corrections were postulated as necessary in a recent article on coupled-channel descriptions of reaction cross sections of excited states which ignores the effects of Pauli and nonlocality in the specification of the effective interaction [41].

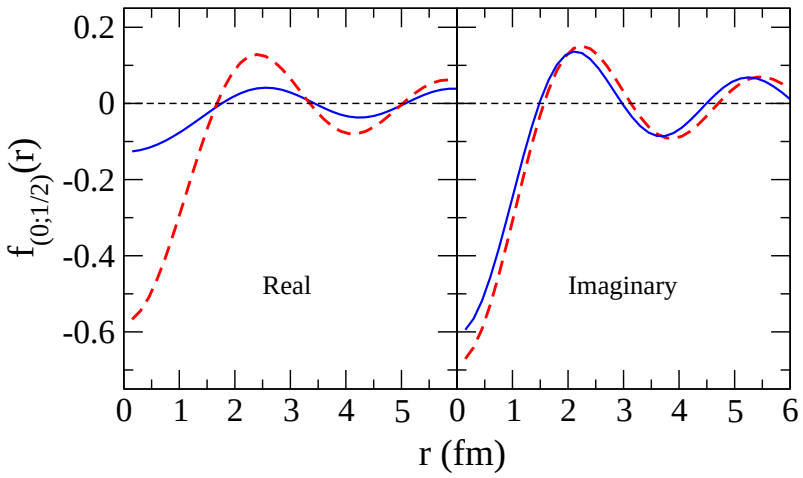

FIG. 8: (Color online) s-wave relative motion wave functions for 40 MeV neutrons on ^{208}Pb. The real and imaginary parts are as indicated with the solid and dashed lines giving the results found using the g-folding and local phenomenological optical model potentials respectively.

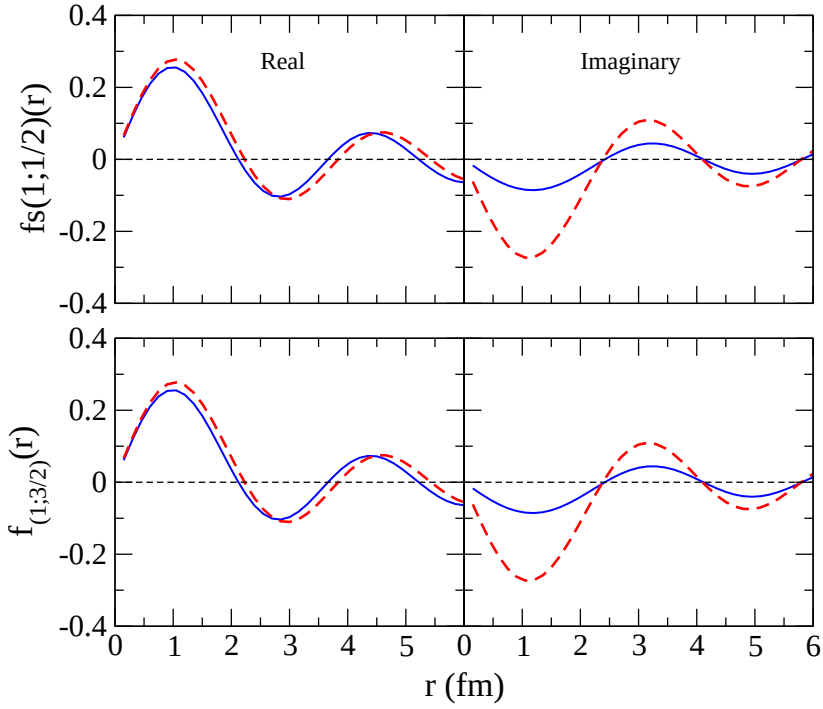

FIG. 9: (Color online) p-wave relative motion wave functions for 40 MeV neutrons on ^{208}Pb. The results for spins $\frac{1}{2}$ and $\frac{3}{2}$ are in the top and bottom segments respectively. Other specifics are as for Fig. 8.

B. Core polarisation

Core polarisation enhancement of calculated cross sections, or form factors, to replicate data is a measure of inadequacy of the structure model used. Such enhancement should be momentum-transfer dependent. That makes using any specified core polarisation from

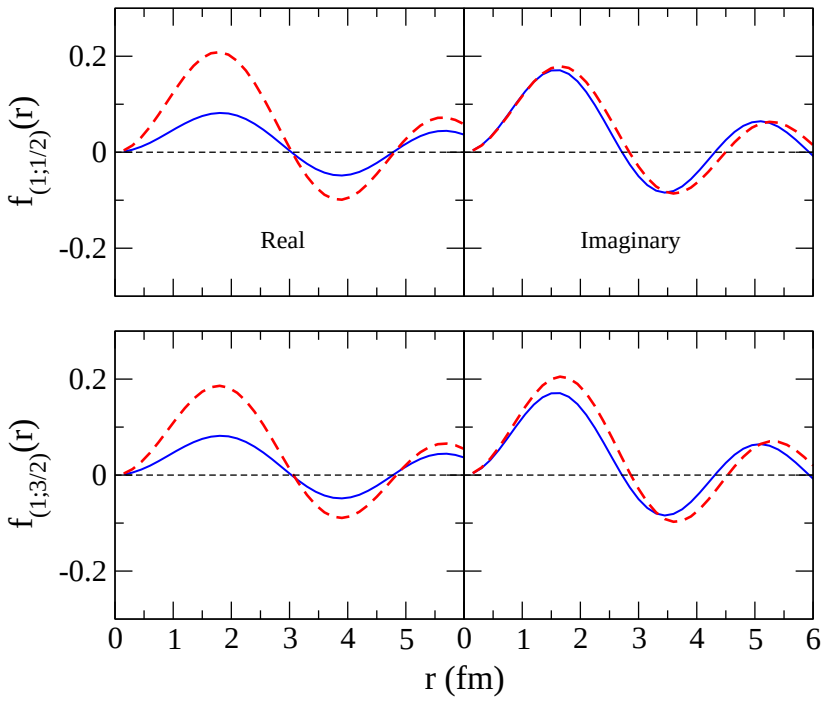

FIG. 10: (Color online) d-wave relative motion wave functions for 40 MeV neutrons on ^{208}Pb. The results for spins $\frac{3}{2}$ and $\frac{5}{2}$ are in the top and bottom segments respectively. Other specifics are as for Fig. 8.

one data set not necessarily the correct one for use with another. For example, to use electromagnetic transition rates (essentially zero momentum quantities) to specify a core polarisation for scattering cross sections typically specified for a range of momentum transfer (~ 0.2 to ~ 2.5 fm^{-1}) is erroneous, as is the reverse.

1. *Core polarization from electromagnetic properties*

Consider the transition between the ground and first excited states in ^{6}Li for which the $B(E2)$ and longitudinal electron scattering form factor are both well known. However, first we need specify in brief the shell models to be used in evaluations of both quantities. More details are given in Ref. [42].

Consider shell model wave functions within the $0\hbar\omega$, $(0+2)\hbar\omega$, and $(0+2+4)\hbar\omega$ model spaces. The choice of model space dictates the choice of interaction. The ones used were the Cohen and Kurath (6-16)2BME interaction (CK) for the complete $0\hbar\omega$ model space, the MK3W interaction for the complete $(0+2)\hbar\omega$ shell model space, and the G-matrix interaction of Zheng *et al.* [43] for the complete $(0+2+4)\hbar\omega$ model space. The shell model wave functions found with each set were used to find the longitudinal inelastic electron scattering form factor to the $3^+;0$ (2.185 MeV) state, amongst others [42]. In Fig. 12, the results found using the $(0+2+4)\hbar\omega$ wave functions are depicted by the solid curves, those with the $(0+2)\hbar\omega$ ones by the dashed curves, and those with the $0\hbar\omega$ model by the dot-dashed curves. In the panel (a), the data are those of Bergstrom *et al.* [46] (circles), of Yen *et al.* [45] (squares), of Bergstrom and Tomusiak [44] (crosses), and Hutcheon and of Caplan [47] (triangles). The form factor, calculated with all shell models, is dominated by the $C2$ component, while the

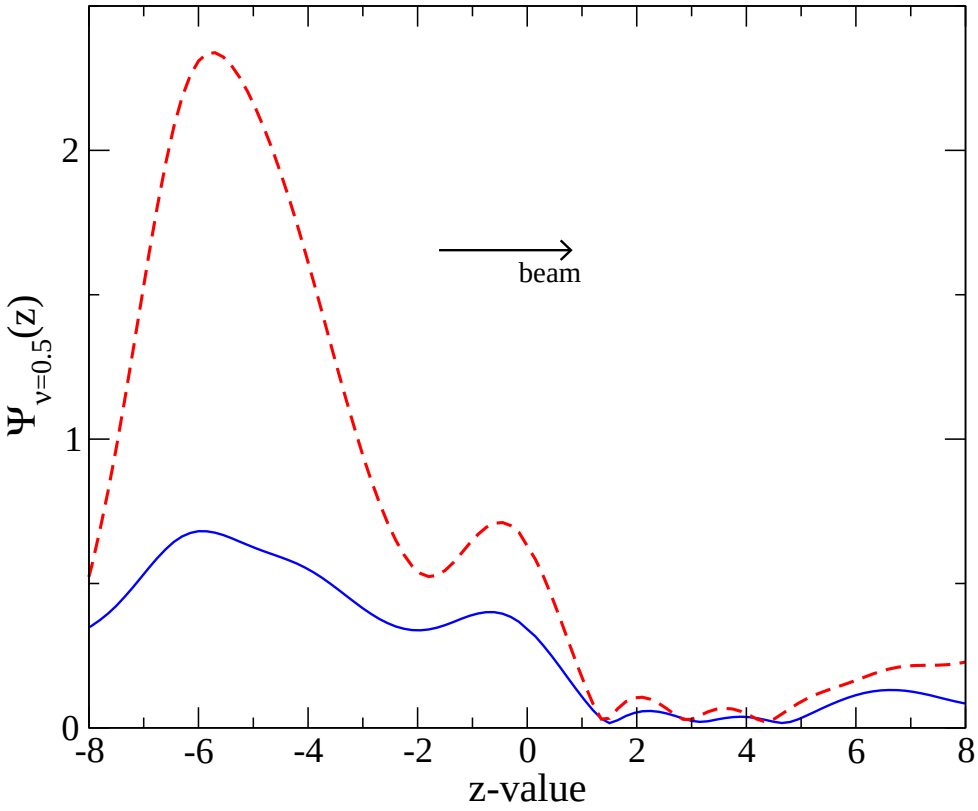

FIG. 11: (Color online) The magnitudes of the complete scattering waves for 40 MeV neutrons on ^{208}Pb along the z axis. The g-folding interaction gave the result shown by the solid curve while that found from the phenomenological optical model is depicted by the dashed curve.

$C4$ component is found to be negligible. With the MK3W and Zheng models, the calculated results reproduce the magnitude of the measured form factor above 1 fm^{-1}. Both have strength from transitions outside of the $0p$ shell which enhance the $C2$ strength. Such are missing in the $0\hbar\omega$ model. The $(0+2+4)\hbar\omega$ model structure is most favoured as there is almost exact agreement with the data in that region of momentum transfer. However, the $B(E2)$ value for the γ-decay of this $3^+_1;0$ state is 9.3 ± 2.1 e^2fm^4, and the values obtained by calculation using the three models of structure are significantly smaller [42]. So far as the γ-decay is concerned, all calculations require a substantial renormalization to reproduce the measured value. That is confirmed by predictions of the electron scattering form factor at low momentum transfer. Below 1 fm^{-1} all of the calculated results are less than observation. Yet that degree of renormalization is not suggested by the results of the calculations of the form factor at higher momentum transfer. While this suggests that the internal (nucleon) dynamics of the nucleus are well described by the inclusion of higher $\hbar\omega$ excitations in the model space, such cannot account for the asymptotics of the structure. At large radii, which most influence scattering at low momentum transfer, the clustering of the wave functions are not reproduced by the shell model in which up to $4\hbar\omega$ excitations are included. That is also why the shell model wave functions also do not give the correct quadrupole moment for ^{7}Li. This deviation of all the calculated results away from the data is illustrated further in the (b) panel of Fig. 12 in which the $B(E2\downarrow, q)$ value for the $3^+;0$ (2.186 MeV) state in ^{6}Li is shown as a function of momentum transfer. These values have been determined from the

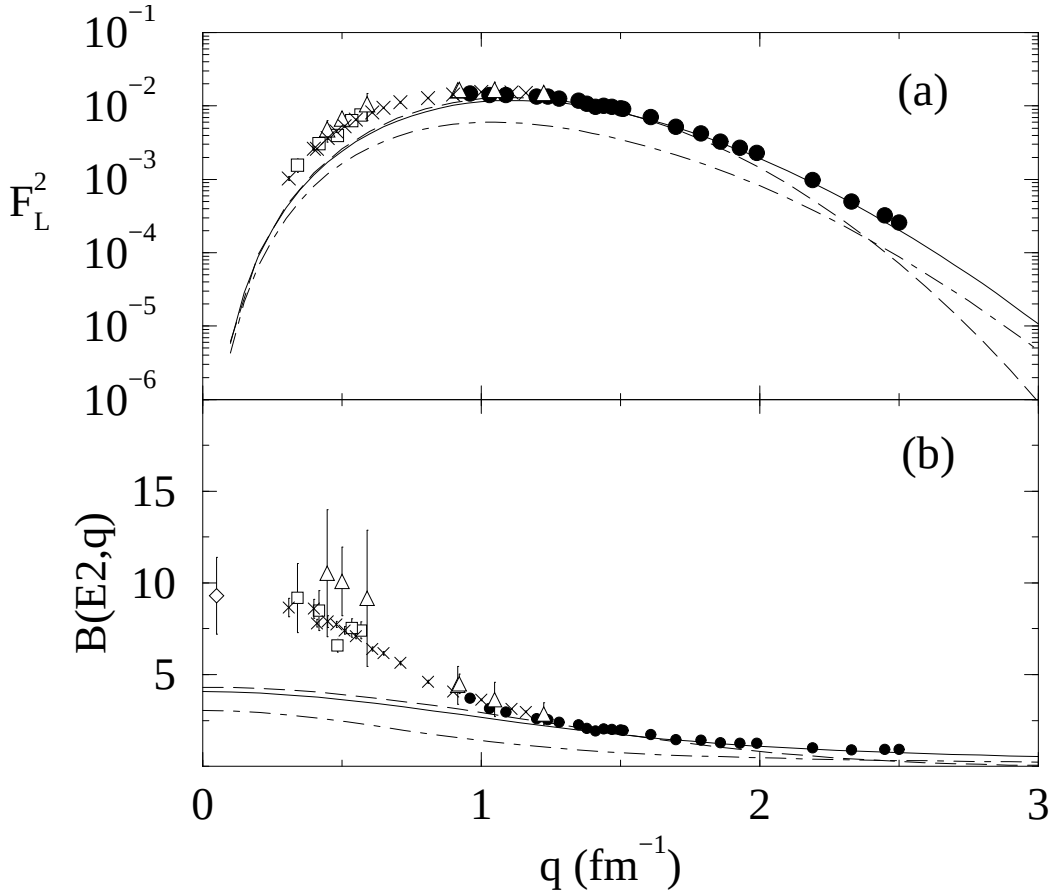

FIG. 12: (a) Longitudinal inelastic electron scattering form factor to the $3^+;0$ (2.186 MeV) state in ^{6}Li, and (b) the $B(E2\downarrow, q)$ values, in units of $e^2\text{fm}^4$, as obtained from the form factor [42]. The data of Bergstrom *et al.* [44] (circles), of Yen *et al.* [45] (squares), of Bergstrom and Tomusiak [46] (crosses), and of Hutcheon and Caplan [47] (triangles) are compared with the results of the calculations. The $B(E2\downarrow)$ value from the associated γ-decay rate is displayed by the diamond data point in (b).

measured and predicted longitudinal inelastic scattering form factors, achieved by removing from the form factor most of the dependence on the momentum transfer according to the transformation of Brown, Radhi, and Wildenthal [48]. The $B(E2\downarrow)$ value is related to the associated γ-decay which is given by the $q \sim 0$ intercept.

2. Core polarization from radial transition form factors

Core polarization has been required in DWIA (distorted wave impulse approximation) analyses of pion inelastic scattering to match calculated cross sections to observed data [49]. Therein, large basis microscopic models of nuclear structure were used to specify the 'collective' form factors for inelastic scattering to the 2_1^+ states in ^{12}C and ^{28}Si. The π-nucleon t-matrices input were fixed by fits to $\pi - N$ elastic scattering phase shifts. All details are given in Ref. [49].

The large basis models of nuclear structure used in Ref. [49], though superseded now,

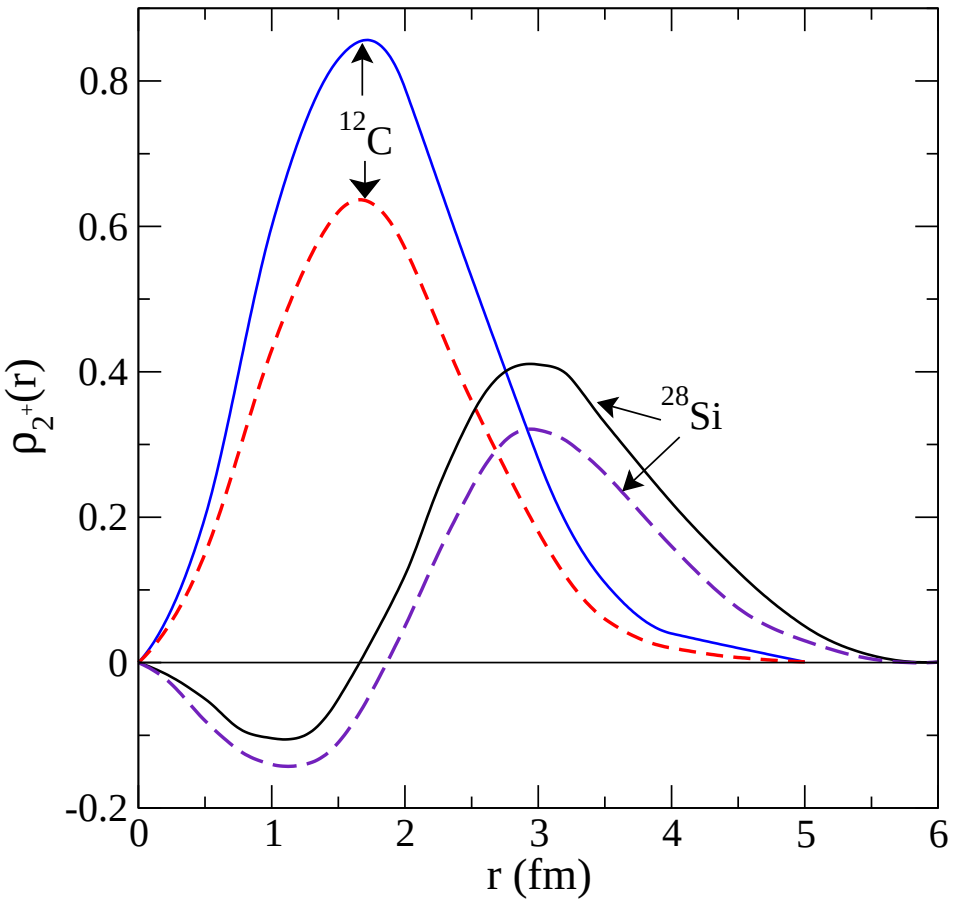

FIG. 13: (Color online) Transition radial densities for the excitation of the 2_1^+ (4.44 MeV) state in ^{12}C (left) and of the 2_1^+ (MeV) state in ^{28}Si.

suffice for the point to be made. For the transition in ^{12}C, a large basis projected Hartree-Fock calculation was made. For the transition in ^{28}Si, large basis Nilsson model wave functions were used. All single nucleon orbits to $4\hbar\omega$ excitation were considered and, from those model structures, transition one-body density matrices (OBDME) were defined. Of those the dominant set of values were in the p-shell for ^{12}C and in the sd-shell for ^{28}Si. Those values are very similar to what was found using the conventional $0\hbar\omega$ shell model for each nucleus. However, the other entries were not trivial and can be considered as the 'core polarization' corrections to the basic $0\hbar\omega$ model values.

With those OBDME, and with harmonic oscillator single nucleon wave functions, radial transition densities for the excitation of the 2_1^+ states from the ground states were determined. They are the transition form factors required in the DWIA evaluations of the pion (inelastic) scattering cross sections. These radial transition densities for both nuclei are shown in Fig. 13.

The solid curves are the transition densities found using the complete set of OBDME from the large basis wave model wave functions. The dashed curves are the densities formed by restricting the sums of OBDME to just the p-shell terms for ^{12}C and just the sd-shell entries for ^{28}Si. Comparison of the two densities for ^{12}C indicates that the 'core polarization' enhances the density profile so that any cross section (essentially the Fourier transform of the transition density) would be simply increased in magnitude consistent with the conventional

usage of polarization charges. In fact the increase is a scale of ~ 1.4 so that a cross section would be increased by a factor ~ 2. However, that is not the case with ^{28}Si. Clearly the addition of the 'core polarization' contributions changes the profile of the transition density, reducing its strength in the region $0 \leq r \leq 2$ fm but increasing the strength at larger radii. The Fourier transforms of the two then will differ, and one can expect so also will the deduced cross sections.

3. The M_n/M_p approach

There are a number of studies, that of Chien and Khoa [50] being a most recent example, in which neutron scattering amplitude scalings were linked to proton ones through electromagnetic properties. Those studies have used the M_n/M_p ratio defined by Bernstein, Brown, and Madsen [51] who recognised that the combined measurements of inelastic hadron and of electromagnetic excitation of the same states in a nucleus could provide a way to probe, simultaneously, the proton and neutron excitations in the transition. They formulated a phenomenological link to specify the ratio of multipole transition moments for protons (M_p) and neutrons (M_n), namely

$$\frac{M_n}{M_p} = \frac{b_p}{b_n}\left[\frac{\delta_h}{\delta_{em}}\left(1 + \frac{b_n}{b_p}\frac{N}{Z}\right) - 1\right], \tag{2}$$

where for the nucleus (Z, N), δ_h is a deformation length to be determined from (p, p') scattering, δ_{em} is the electromagnetically defined deformation length, and b_n, b_p are interaction strengths of the incident proton with target neutrons and protons respectively.

The multipole transition elements themselves are defined by

$$M_{p(n)} = \left\langle J_f \left\| \sum_{i \in p(n)} r_i^\lambda Y_\lambda(\Omega_i) \right\| J_i \right\rangle = \int_0^\infty \rho_\lambda^{p(n)}(r)\ r^{\lambda+2}\ dr, \tag{3}$$

where $\rho_\lambda^{p(n)}(r)$ are transition densities as described in the preceding subsection and λ is the multipolarity of the transition.

Usually the $B(E2)$ values are used [52, 53], though in Ref. [50], it was the $B(E2)$ values from the 2_1^+ state decays from proton-rich ^{18}Ne and ^{20}Mg to compare with their mirror systems in the neutron-rich Oxygen isotopes. Iwasa *et al.* [53] noted that there could be systematic uncertainties, possibly caused by insufficient knowledge of the mechanism of proton inelastic scattering. As the proton multipole transition moment is determined solely by electromagnetic data, the approach negates any contributions to M_p from the effective NN interaction. The process is not a reliable way to assess details of nuclear structure. Likewise it should not be used to specify $B(E2)$ values from inelastic scattering cross sections from hydrogen targets, as has been considered for the spectra of radioactive ions.

Though many of the problems with this approach have already discussed, it is worthwhile listing them for emphasis. First the $B(E2)$ are essentially a zero momentum transfer property which, if a perfect model of structure were available, would depend upon, only the proton transition density, with

$$B(E2) = \frac{1}{(2J_i + 1)} M_p^2 \tag{4}$$

in units of $e^2\text{fm}^4$. It is questionable therefore to use this to compare data from a mirror system, for example the $B(E2)$ from ^{20}Mg to that in ^{20}O. Of course, there are mirror symmetries in spectra of mirror nuclei, but save for the weak Coulomb displacement energies, the symmetry is due to charge independence of the nuclear force. However, at first order, the neutrons in a nucleus do not contribute to $B(E2)$ values. They do contribute in so far as they influence proton distributions through the NN interactions being stronger for a pn pair than with like nucleons, but not directly otherwise.

Hadron inelastic scattering, of protons in particular, have measured cross sections usually in a finite range of momentum transfer values that are not very close to zero. That is particularly so with the inverse kinematic problem of radioactive ion beams (RIBs) scattering from hydrogen targets. As noted previously, there is a better match in momentum transfer values if one compares electron form factors with (p, p') cross sections, but experimental data from electrons scattering with RIBs, either a cross beam by or using a SCRIT (self contained radioactive ion target) experiment [54] are yet to be realised.

As stated earlier, perhaps the biggest problem of using the M_n/M_p ratio method is that it assumes that the proton scattering transition moment may be solely determined by fits to electromagnetic data. The allowance for specific nuclear interaction effects, the role of the Pauli principle in making the actual transition amplitudes creating exchange amplitudes which often have serious interference with the direct ones, and the effects of nuclear distortion in the relative motion wave functions, are all missing in the identifications given in Eqs. (2) and (3). These reasons bring into question the conclusions made in the recent article [50] dealing with neutron transition strengths of 2_1^+ states in the neutron-rich Oxygen isotopes. That is especially so since the assessment of the structure of those isotopes specified by a large basis shell model and their use in analyses of the scattering cross sections of those RIBs from hydrogen targets existed in the literature [55].

IV. CONCLUSIONS

Of course, if only a set of elastic scattering phase shifts that lead to a quality fit to elastic scattering and total reaction cross-section data are required, then any prescription that does so can be used. But usually the elastic scattering data and its fit are but a prelude to what is sought. By itself, one might seek to make conclusions about matter distributions in a nucleus from an assessment of elastic scattering data. To do so, however, one need use a more detailed theory of that scattering than usually has been the case. At least the Pauli principle and the nonlocality of the NA optical potential that it creates must be taken into account, and those nonlocalities should not be approximated with some local equivalent form. There is no need to do so now as the suite of programs DWBA98 and above, facilitate such analyses. The effect of medium corrections in the projectile nucleon – target nucleon effective interactions can be handled in those programs as well, and a utilitarian prescription for those effective interactions has been published [3]. The computer programs that generate the effective interactions by those means are available upon request.

Often the associated relative motion (distorted) wave functions are required, such as in DWA analyses of inelastic, charge and particle exchange reaction data. Those analyses seek conclusions regarding structures of excited states and of processes involved. An example was the use to constrain double beta decay rates [56]. The problems regarding approximations leading to effective local interaction forms of the optical potential are accentuated in all such analyses with the radial properties of the distorted waves from a nonlocal interaction being

quite different through the nuclear transition interaction region (interior and surface of the nucleus) from those of an "equivalent" local optical potential with which a good fit to elastic scattering data was found.

While this study has centred upon the problems associated with an NA optical potential and its use in inelastic scattering analyses, many of the same issues attend analyses of nucleus-nucleus scattering data and conclusions about structure drawn from them.

Acknowledgments

SK acknowledges support from the National Research Foundation of South Africa.

---

[1] H. Bethe, Phys. Rev. **57**, 1125 (1940).
[2] A. K. Kerman, H. McManus, and R. M. Thaler, Ann. Phys. (N.Y.) **8**, 551 (1959).
[3] K. Amos, P. J. Dortmans, H. V. von Geramb, S. Karataglidis, and J. Raynal, Adv. in Nucl. Phys. **25**, 275 (2000), (and references contained therein).
[4] J. P. Jeukenne, A. Lejeunne, and C. Mahaux, Phys. Rep. **25**, 83 (1976).
[5] E. Becheva et al., Phys. Rev. Lett. **96**, 012501 (2006).
[6] D. R. Lun, M. Eberspächer, K. Amos, W. Scheid, and S. J. Buckman, Phys. Rev. A **58**, 4993 (1998).
[7] A. Lovell and K. Amos, Phys. Rev. C **62**, 064614 (2000).
[8] H. O. Meyer, P. Schwandt, W. W. Jacobs, and J. R. Hall, Phys. Rev. C **27**, 459 (1983).
[9] L. J. Allen, K. Amos, and P. J. Dortmans, Phys. Rev. C **49**, 2177 (1994).
[10] S. V. Stepansov et al., Phys. Letts. **B 542**, 35 (2002).
[11] P. K. Deb and K. Amos, Phys. Rev. C **62**, 024605 (2000).
[12] R. A. Arndt, L. D. Roper, R. A. Bryan, R. B. Clark, B. J. ver West, and P. Signell, Phys. Rev. D **28**, 97 (1983).
[13] M. M. Nagels, T. A. Rijken, and J. J. de Swart, Phys. Rev. D **17**, 768 (1978).
[14] M. Lacombe, B. Loiseau, J. M. Richard, R. V. Mau, J. Côté, P. Pirés, and R. de Tourreil, Phys. Rev. C **21**, 861 (1980).
[15] R. Machleidt, K. Holinde, and C. Elster, Phys. Rep. **149**, 1 (1987).
[16] H. V. von Geramb, ed., *Microscopic Optical Potentials, Proc. of the Hamburg Topical Workshop*, vol. 89 of *Lecture Notes in Physics* (Springer-Verlag, Berlin, 1979).
[17] P. Schwandt, in *Proc. Int. Workshop on Medium Energy Nucleons in Nuclei*, edited by H. O. Meyer (AIP, New York, 1983), vol. 97 of *AIP Conf. Proc.*
[18] L. Ray, G. W. Hoffmann, and W. R. Coker, Phys. Rep. **212**, 223 (1992).
[19] G. R. Satchler, *Direct Nuclear Reactions*, International series of monographs on physics (Clarendon, New York, 1983), 68th ed.
[20] H. Feshbach, *Theoretical Nuclear Physics: Nuclear Reactions* (Wiley, London, 1992).
[21] P. E. Hodgson, *The Nucleon Optical Potential* (World Scientific, Singapore, 1994).
[22] L. Ray, Phys. Rev. C **41**, 2816 (1990).
[23] H. Sakaguchi et al., Phys. Rev. C **26**, 944 (1982).
[24] S. Karataglidis, K. Amos, B. A. Brown, and P. K. Deb, Phys. Rev. C **65**, 044306 (2002).
[25] M. Ibaraki et al., Nucl. Instrum. and Meth. in Phys. Res. **A 446**, 536 (2000).

[26] W. T. H. van Oers et al., Phys. Rev. C **10**, 307 (1974).
[27] R. W. Finlay, J. R. M. Annand, T. S. Cheema, J. Rapaport, and F. S. Dietrich, Phys. Rev. C **30**, 796 (1984).
[28] K. Amos, L. Canton, G. Pisent, J. P. Svenne, and D. van der Knijff, Nucl. Phys. **A728**, 65 (2003).
[29] L. Canton, G. Pisent, J. P. Svenne, K. Amos, and S. Karataglidis, Phys. Rev. Lett. **96**, 072502 (2006).
[30] K. Amos, S. Karataglidis, D. van der Knijff, L. Canton, G. Pisent, and J. P. Svenne, Phys. Rev. C **72**, 064604 (2005).
[31] H. V. von Geramb, K. Amos, R. Sprickmann, K. T. Knöpfle, M. Rogge, D. Ingham, and C. Mayer-Böricke, Phys. Rev. C **12**, 1697 (1975).
[32] J. A. Tostevin, F. M. Nunes, and I. J. Thompson, Phys. Rev. C **63**, 024617 (2001).
[33] A. Deltuva, A. M. Moro, E. Cravo, F. M. Nunes, and A. C. Fonseca, Phys. Rev. C **76**, 064602 (2007).
[34] F. Skaza et al., Phys. Lett. **619B**, 92 (2005).
[35] R. S. Mackintosh and N. Keeley, Phys. Rev. C **81**, 034612 (2010).
[36] E. Khan et al., Nucl. Phys. **A694**, 103 (2001).
[37] P. K. Deb, B. C. Clark, S. Hama, K. Amos, S. Karataglidis, and E. D. Cooper, Phys. Rev. C **72**, 014608 (2005).
[38] J. Raynal, *computer code dwba70* (1981), (NEA 1209/02).
[39] N. Austern, Phys. Rev. **137**, B752 (1965).
[40] H. Fiedeldey, Nucl. Phys. **77**, 149 (1966).
[41] T. Kawano, P. Talou, J. E. Lynn, M. B. Chadwick, and D. G. Madland, Phys. Rev. C **80**, 024611 (2009).
[42] S. Karataglidis, B. A. Brown, K. Amos, and P. J. Dortmans, Phys. Rev. C **55**, 2826 (1997).
[43] D. C. Zheng, B. R. Barrett, J. P. Vary, W. C. Haxton, and C.-L. Song, Phys. Rev. C **52**, 2488 (1995).
[44] J. C. Bergstrom, U. Deutschmann, and R. Neuhausen, Nucl. Phys. **A327**, 439 (1979).
[45] R. Yen, L. S. Cardman, D. Kalinsky, J. R. Legg, and C. K. Bockelman, Nucl. Phys. **A235**, 135 (1974).
[46] J. C. Bergstrom and E. L. Tomusiak, Nucl. Phys. **A262**, 196 (1976).
[47] R. M. Hutcheon and H. S. Caplan, Nucl. Phys. **A127**, 417 (1969).
[48] B. A. Brown, R. Radhi, and B. H. Wildenthal, Phys. Rep. **101**, 313 (1983).
[49] K. Amos and L. Berge, Phys. Lett. **127B**, 299 (1983).
[50] N. D. Chien and D. T. Khoa, Phys. Rev. C **79**, 034314 (2009).
[51] A. M. Bernstein, V. R. Brown, and V. A. Madsen, Comments Nucl. Part. Phys. **11**, 203 (1981).
[52] F. Marechal et al., Phys. Rev. C **60**, 034615 (1999).
[53] N. Iwasa et al., Phys. Rev. C **78**, 024306 (2008).
[54] T. Suda and M. Wakasugi, Prog. Part. Nucl. Phys. **55**, 417 (2005).
[55] S. Karataglidis, Y. J. Kim, and K. Amos, Nucl. Phys. **A 793**, 40 (2007).
[56] K. Amos, A. Faessler, and V. Rodin, Phys. Rev. C **76**, 014604 (2007).